

Induced Smectic-G Phase through Intermolecular Hydrogen Bonding, Part XII: Thermal and Phase Behaviour of *p*-aminobenzonitrile: *p*-*n*-alkoxybenzoic acids

P. A. Kumar, V. G. K. M. Pisipati, A. V. Rajeswari^a, and S. Sreehari Sastry^a

Centre for Liquid Crystal Research and Education (CLCRE), Faculty of Physical Sciences, Nagarjuna University, Nagarjunanagar 522 510, India

^a Department of Physics, Nagarjuna University, Nagarjunanagar 522 510, India

Reprint requests to Prof. V. G. K. M. P.; Fax: +91-0863-235900; E-mail: venkata_pisipati@hotmail.com

Z. Naturforsch. **57a**, 184–188 (2002); received January 16, 2002

New liquid crystalline compounds involving intermolecular hydrogen bonding between mesogenic *p*-*n*-alkoxybenzoic acids (*n*ABA) (where *n* denotes the alkoxy carbon number varying from propyl- to decyl- and dodecyl-) and *p*-aminobenzonitrile (ABN) are synthesized. The thermal and phase behaviour of these materials is studied by Thermal Microscopy and Differential Scanning Calorimetry. A detailed IR spectral investigation in solid and solution states confirms the formation of H-bonding between cyano and –COOH groups of ABN and *n*ABA, respectively. Comparative thermal analyses of both free *p*-*n* alkoxybenzoic acids and H-bonded complexes suggest the induction of smectic-G phase in all the complexes.

Key words: H-bonding; *n*ABA; ABN; Smectic-G.

Introduction

Supramolecular liquid crystals, obtained through hydrogen-bonding of complementary molecules, have extensively been investigated in recent years. Following the well-established examples of liquid crystal formation through dimerization of aromatic carboxylic acids [1, 2], several classes of compounds have been reported, including conventional liquid crystals [3–9], supramolecular polymer networks [10–13], and ferroelectric liquid crystals [14–17] formed by the interaction of complementary molecules, the liquid crystalline behaviour of which is crucially dependent on the structure of the resulting supramolecular system. It is now well-established that for the formation of liquid crystalline materials through hydrogen bonding, the complementarity of the interacting components coupled with the directionality of the hydrogen bonds are the main (but not the only) factors contributing to liquid crystallinity [18]. In fact, it has been widely accepted that the proton donor and acceptor capabilities of the atoms of the functional groups involved in the hydrogen bonding contribute remarkably to the occurrence of new phases and their thermal stability. Despite their low bond activation energies, these non-covalent interactions show a profound impact on thermal and physical properties such as melting points, heats of vaporization, mesomorphic behaviour, etc.

In continuation of our systematic investigation of H-bonded liquid crystals comprising different proton and acceptor groups [19–23], the present communication deals with the synthesis and phase behaviour of a new series of liquid crystalline systems involving intermolecular hydrogen bonding between *p*-*n*-alkoxybenzoic acids (*n*ABA) and *p*-aminobenzonitrile (ABN). The molecular structure of the ABN:*n*ABA series is represented in Figure 1.

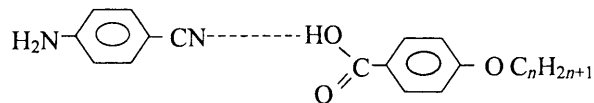


Fig. 1. Molecular structure of the ABN:*n*ABA series

Experimental

Materials and Methods

The compounds *p*-*n*-alkoxybenzoic acids and *p*-aminobenzonitrile were supplied by Frinton laboratories, New Jersey and Kodak Chemical Company, USA, respectively. All the solvents used in the present work are of E. Merck grade and are used as such without further purification. The solid state (KBr) IR spectra were recorded on a Perkin-Elmer (spectrum BX series) FT-IR

spectrometer. The optical textural observations were carried out by thermal microscopy (Olympus BX 50) equipped with an optical display (DP-10). The Differential Scanning thermograms were recorded on a Perkin-Elmer DSC 7.

Intermolecular Hydrogen Bonding Complexes

The intermolecular H-bonding complexes, ABN:*n*-ABA were synthesized by refluxing together *p*-alkoxybenzoic acids (~ 1.3 g/6.0 mmol) and ABN (0.7 g/6.0 mmol) in 20 ml of pyridine under constant stirring at 80 °C for ~ 2 h. The volume of the resultant homogeneous mixture was then reduced to dryness by removing the excess pyridine under a controlled vacuum filtration. The white crystalline products were dried and recrystallized from a hot dichloromethane solution. The yields obtained are ~ 1.9 g (81%).

Results and Discussion

IR Spectra

The solid state (KBr) IR spectra of *n*ABA, ABN, and their H-bonded complexes were recorded at room temperature. The spectra of free *p*-*n*-alkoxybenzoic acids show two sharp bands at 1685 and 1695 cm⁻¹ due to the $\nu(\text{C}=\text{O})$ mode and a strong intense band at 3032 cm⁻¹ assigned to the $\nu(\text{OH})$ mode of the carboxylic acid group. This doubling nature of the carbonyl stretching mode may be attributed to the existence of dimeric benzoic acid at room temperature [24]. However, the corresponding spectra recorded in solution (chloroform) show an intense band at 1712 cm⁻¹, suggesting stabilization of the monomeric form of benzoic acid in solution. To avoid further complications due to inter/intramolecular hydrogen bonding, the spectra of the complexes were compared with the free benzoic acids recorded in solution state.

The IR spectrum of the free-ABN moiety exhibits an intense band at ~ 1602 cm⁻¹ due to the $\nu(\text{C}=\text{N})$ mode, and two medium intense bands at 3364 and 3473 cm⁻¹ assigned to symmetric and asymmetric stretching modes of the -NH₂ group [24].

The infrared frequencies of ABN:*n*ABA complexes show (Table 1) a sharp band at ~ 1680 cm⁻¹ due to the $\nu(\text{C}=\text{O})$ mode of the benzoic acid moiety, which suggests its monomeric nature upon complexation. When compared to the free-*n*ABA spectra, the ABN:*n*ABA complexes show bathochromic shifts (~ 25 cm⁻¹) in the $\nu(\text{C}=\text{O})$ mode of the benzoic acid moiety and

Table 1. IR spectral data (cm⁻¹).

Compound	$\nu(\text{NH})_{\text{sym}}$	$\nu(\text{NH})_{\text{asym}}$	$\nu(\text{CN})$	$\nu(\text{CO})_{\text{acid}}$	$\nu(\text{OH})_{\text{acid}}$
OBA (KBr)	–	–	–	1685,1695	3032
OBA (CH ₃ Cl)	–	–	–	1712	3040
ABN	3364	3473	1602	–	–
ABN: <i>n</i> ABA (<i>n</i> = 8)	3362	3471	1625	1687	3019

OBA = *p*-Octyloxybenzoic acid.

hypsochromic shifts (~ 25 cm⁻¹) in the $\nu(\text{C}=\text{N})$ mode of the ABN moiety. These shifts strongly suggest the formation of intermolecular H-bonding between the -COOH group and the *cyano* group. Moreover, the band associated with the $\nu(\text{OH})$ mode of the carboxylic acid group suffered a bathochromic shift upon complexation, which strongly supports the existence of H-bonding. The non-involvement of the terminal -NH₂ group of the ABN moiety in hydrogen bonding is invoked on the basis of the unaltered appearance of the bands associated with the stretching modes of this group in the H-bonded compounds (Table 1).

Thermal and Phase Behaviour

The phases and their transition temperatures (Table 2) were determined by textural observations [25] under a polarizing microscope equipped with a temperature control system at a scan rate of 0.1 °C/minute. The *p*-*n*-alkoxybenzoic acids exhibit the nematic (marble) phase of the lower homologues (*n* = 3 to 6) and the smectic-C (schilieren) phase of the higher members of the series.

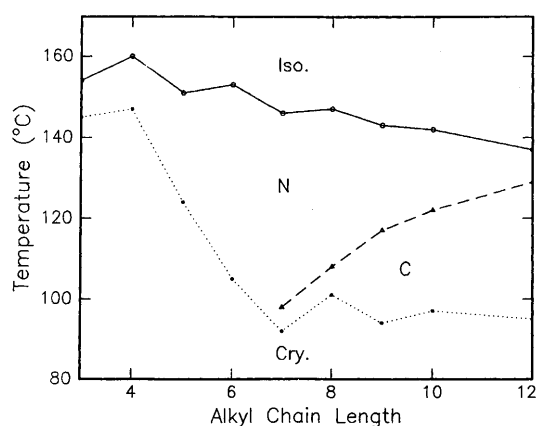
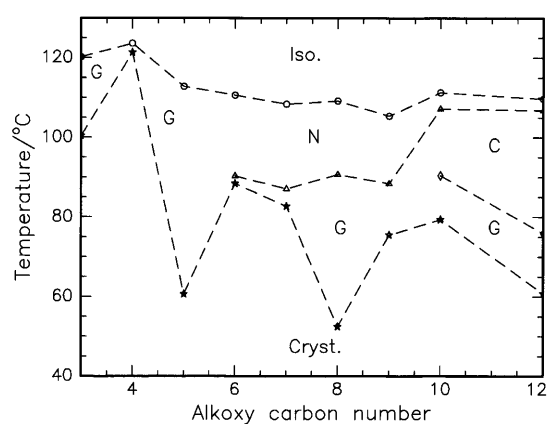
On cooling the isotrope melt, the higher homologues (*n* = 6 to 10 and 12) of the present series exhibit a threaded nematic texture which is developed from nematic droplets on slow cooling. On further cooling, formation of schilieren, assigned to the smectic-C phase, is observed in compounds VIII and IX (*n* = 10 and 12). A smooth multicolored mosaic texture characteristic of smectic-G phase [25] is induced in all the compounds. Further, the lower homologues (*n* = 3 to 5) exhibit a direct isotropic to smectic-G phase transition with quenching of the nematic phase of free *p*-*n*-alkoxybenzoic acids. The phase transition temperatures observed through thermal microscopy were found to be in reasonable agreement with the corresponding DSC thermograms (Table 2).

The phase diagrams were constructed from the transition temperatures observed by thermal microscopy in

Table 2. Thermal and phase behaviour of ABN:*n*ABA compounds.

ABN: <i>n</i> ABA (<i>n</i>)	Phase variant	Phase transition temperatures/°C of TM and [DSC ($\Delta H/J/gm$)]			
		Iso.-N/G	N-C/G	C-G	G-Cryst.
I (3)	G	120.2 [119.4 (29.4)]			100.4 [98.1 (22.5)]
II (4)	G	123.6 [121.6]*			121.3 [120.3 (32.1)]
III (5)	G	112.8 [107.1]			60.6 [-]
IV (6)	NG	110.6 [104.2 (4.3)]	90.3 [88.8 (33.1)]		88.4 [-]
V (7)	NG	108.4 [105.8 (9.4)]	87.1 [84.1 (37.3)]		82.7 [79.3 (47.5)]
VI (8)	NG	109.2 [111.1 (6.4)]	90.7 [92.3 (37.3)]		52.5 [47.5 (37.2)]
VII (9)	NG	105.4 [102.4 (0.8)]	88.4 [84.5 (20.2)]		75.5 [63.4 (52.5)]
VIII (10)	NCG	111.3 [109.7 (0.8)]	107.2 [105.5 (1.2)]	90.4 [88.5 (22.4)]	79.4 [72.0 (16.7)]
IX (12)	NCG	109.7 [111.9]*	106.8 [109.8 (23.0)]	75.9 [79.2 (25.5)]	60.8 [66.0 (56.7)]

* Transition peaks are not well resolved.

Fig. 2. Phase diagram of *p-n*-alkoxybenzoic acids.Fig. 3. Phase diagram of ABN:*n*ABA.

the cooling cycle. Figures 2 and 3 illustrate the phase behaviour of the free *n*ABA and the ABN:*n*ABA series, respectively.

A glance at Fig. 3 reveals that the compounds I to III exhibit direct isotropic to smectic-G transitions with simultaneous quenching of nematic phase when com-

pared to free *p-n*-alkoxybenzoic acids. Further, wide thermal ranges ($\sim 40^\circ\text{C}$) of this induced phase are noticed for the compounds III and VI ($n = 5$ and 8). The thermal ranges of the induced phase are stabilized in the higher members of the series. It is interesting to add that compound II shows a very narrow range of smectic-G

phase. The stabilization of this induced phase in the higher members clearly signifies the important role of H-bonding formed between the electron rich terminal *cyano* group and the terminal carbon of *n*ABA. When compared with the phase behaviour of the reported series of 2-amino-5-chloropyridine (ACP):*n*ABA [21], it is observed that there is a gradual decrease of the thermal range of this phase in the higher homologues. This observation provides substantial evidence towards the effective role of the non-mesogenic moiety, ABN, on the phase behaviour of the present series. It is worth mentioning that the thermal distribution of induced smectic-G phase in the reported series derived from *p*-alkoxybenzoates [19, 20] shows a non-uniform trend. This, however, confirms the significant contribution of the *p*-aminobenzonitrile moiety to the phase behaviour of the present series.

It is further noticed that the nematic and smectic-G phases have their maximum thermal ranges in complex VI (with $n = 8$) in this series. Figures 2 and 3 reveal the quenching of smectic-C phase in the present series (except $n = 10$ and 12), where this is the dominant phase in the free *n*ABA. A stabilization of the nematic phase in terms of wide thermal spans is found at lower temperatures for the compounds IV to VIII ($n = 6$ to 10) of the present series when compared to the free acids. However, the middle members of the series (compounds IV–VII) show nematic and smectic-G as dominant mesophases. The present series also shows wide liquid crystalline thermal ranges with a well stabilized induced phase (smectic-G) when compared with its analogous series of complexes, ACP:ABA [21] and 2-(*p*-*n*-nonyloxybenzylidene-*imono*)-5-chloropyridine (NICP):ABA [22]. In fact, the thermal distribution

among the nematic and smectic-G phases in the middle members of this series is also present in the tilted phases (smectic-C and smectic-G) of the higher members. Nevertheless, the transition temperatures across the series show the odd-even effect.

Conclusion

Comparative thermal studies on the present series reveal that a smectic-G phase is induced in all the complexes. A possible explanation of the induction of this new phase may be molecular contributions originated from the intermolecular hydrogen bonding between the electron rich terminal cyano and –COOH groups. Further, new phase variants, viz. G, NG, and NCG in the present series may be due to the presence of the terminal –NH₂ group, which in turn leads to a steric repulsive effect and promotes the stabilization of the induced phase. Moreover, the significant impact of the *cyano* group as proton acceptor on the phase behaviour in terms of wide thermal spans of induced phase may be realized comparing the phase behaviour with analogous series, where –OH/pyridine-nitrogen serves as a proton acceptor.

Acknowledgements

This work is supported by the Council for Scientific and Industrial Research (No: 13(7544-A)/Pool), University Grants Commission (under Faculty Improvement Program) and the Department of Science and Technology (Grant No: SP/S2/M-45/94), New Delhi. The authors are grateful to Prof. K. G. Subhadra, Kakatiya University, Warangal, for recording the IR spectra.

- [1] G. W. Gray, *Molecular Structure and the Properties of Liquid Crystals*, Academic Press, London 1962, p. 163 and references cited therein.
- [2] H. Kelker and R. Hatz, *Hand Book of Liquid Crystals*, Verlag Chemie, Weinheim 1980, p. 59 and references cited therein.
- [3] T. Kato and J. M. J. Frechet, *J. Amer. Chem. Soc.* **111**, 8533 (1989).
- [4] Z. Sideratov, C. M. Paleoes, and A. Skoulios, *Mol. Cryst. Liq. Cryst.* **265**, 2585 (1995).
- [5] P. Weisslaw, E. Gorecka, A. Krowczynski, D. Pocicha, J. Szydłowska, J. Przdmojski, and Li Chen. *Liq. Cryst.* **21**, 885 (1996).
- [6] Y. Tian, X. Xu, Y. Zhao, X. Tang, and T. Li, *Liq. Cryst.* **22**, 87 (1997).
- [7] A. Treybig, H. Bernhardt, S. Diele, W. Weissflog, and H. Kresse, *Mol. Cryst. Liq. Cryst.* **293**, 7 (1997).
- [8] E. B. Barmatov, Y. Bobrovsky, M. V. Barmatova, and V. P. Shibaev, *Liq. Cryst.* **26**, 581 (1999).
- [9] H. O. Limin, X. Chen, and G. E. Zhou, *Liq. Cryst.* **26**, 1053 (1999).
- [10] T. Kato and M. J. Frechet, *Macromol. Symp.* **98**, 311 (1995).
- [11] S. Abed, S. Boileau, L. Bouteiller, J. R. Caille, N. Lacoudre, D. Teyssie, and J. M. Yu, *Polym. Mater. Sci. Eng.* **76**, 45 (1997).
- [12] L. C. Ming and C. A. Griffin, *Macro. Mol. Symp.* **117**, 281 (1997).
- [13] Hong-cheulin, Chung-Wen Ko, K. Guo, and Tze-Wen-cheng, *Liq. Cryst.* **26**, 613 (1999).
- [14] L. J. Yu, *Liquid Crystals* **14**, 1303 (1993).
- [15] T. P. Myasnikova, N. I. Chernova, and M. V. Loseva, *Ferroelectrics* **174**, 107 (1995).

- [16] Tian Yan Qing, X. Xu, Y. Y. Zhao, X. Tang, F. Su, X. U. Zhao, and E. Zhou, *Liq. Cryst.* **19**, 295 (1995).
- [17] K. Hideyuki, T. Kato, U. Toshiyuki, S. Ujiie, U. Kumar, J. M. J. Frechet, D. W. Bruce, and D. J. Price, *Liq. Cryst.* **21**, 25 (1996).
- [18] C. M. Paleos and D. Tsiourvas, *Liq. Cryst.* **28**, 1127 (2001) and references cited therein.
- [19] P. A. Kumar, M. Srinivasulu, and V. G. K. M. Pisipati, *Liq. Cryst.* **26**, 859 (1999).
- [20] P. Swathi, P. A. Jumar, and V. G. K. M. Pisipati, *Liq. Cryst.* **27**, 665 (2000).
- [21] P. Swathi, S. Sreehari Sastri, P. A. Kumar, and V. G. K. M. Pisipati, *Mol. Cryst. Liq. Cryst.* **365**, 523 (2000).
- [22] M. Srinivasulu, P. V. V. Satyanarayana, P. A. Kumar, and V. G. K. M. Pisipati, *Liq. Cryst.* **28**, 1321 (2001); *Mol. Matter* 2001 (in press).
- [23] P. Swathi, P. A. Kumar, and V. G. K. M. Pisipati, *Liq. Cryst.* **28**, 1163 (2001); *Mol. Matter* 2001 (in press). This is Part XI of the series.
- [24] K. Nakamoto, *Infrared and Raman Spectra of Inorganic and Coordination Compounds*. 4th edition, Interscience, New York 1978, and references cited therein.
- [25] G. W. Gray and J. W. G. Goodby, *Smectic Liquid Crystals: Textures and Structures*, Leonard Hill, London 1984.